REAL-TIME TRANSIENT STABILITY STATUS PREDICTION SCHEME AND COMPARATIVE ANALYSIS OF THE PERFORMANCE OF SVM, MLPNN AND RBFNN

Emmanuel Asuming **FRIMPONG**[1], Philip Yaw **OKYERE**[1], Johnson **ASUMADU**[2]
[1]*Kwame Nkrumah University of Science and Technology, Kumasi, Ghana*
[2]*Western Michigan University, Kalamazoo, Michigan, USA*
[1]*eafrimpong.soe@knust.edu.gh,* [2]*pyokyere.soe@knust.edu.gh,* [3] *johnson.asumadu@wmich.edu*

Keywords: neural networks, out-of-step, support vector machine, transient stability

Abstract*:* This paper presents a simple and effective technique for real-time prediction of transient stability status following a large disturbance and compares the performance of three artificial intelligence (AI) techniques commonly employed as decision making tools. The (AI) techniques compared are support vector machine (SVM), multilayer perceptron neural network (MLPNN), and radial basis function neural network (RBFNN). The stability status prediction scheme samples rotor angles of all system generators and extracts the absolute value of the first sampled rotor angle value of each generator. The extracted absolute rotor angle value of all generators are summed and fed as input to a decision tool. The scheme was tested using simulations carried out on the IEEE 39-bus test system. One hundred percent prediction accuracy was obtained when SVM and MLPNN were each employed as decision tools. The use of the RBFNN as decision tool resulted in only sixty-three percent prediction accuracy.

1. INTRODUCTION

Large disturbances such as faults on transmission lines endanger stability of power systems and can lead to wide-scale system outages. This is particularly so when protection schemes are not able to effectively respond to fault conditions. For example, the August 14, 2003 blackouts that occurred in United States and Canada were mainly due to the combined effect of large disturbances and ineffective system protection [1].

Power system faults pose the greatest threat to the maintenance of stability. Severe disturbances could cause large separation of the rotor angles between generators or groups of generators leading to eventual loss of synchronism [2]. The post-disturbance stability status of a system depends on the pre-disturbance system operating condition, the form of disturbance, and the post-disturbance network configuration [3]. Special protective systems (SPSs) which are event based control systems have been developed to address transient instability. SPSs activate controls in response to occurrence of some pre-identified set of disturbances. They are however complicated and expensive; any modifications to the power system requires alteration of their control logic [4].

Researchers have therefore come up with a number of techniques for early detection and prediction of transient instability [2], [4]-[12]. These techniques hinge on the combined ability of phasor measurement units (PMUs) and global positioning system (GPS) to provide real-time capture and transmission of power system data to a centralized location.

Critical issues in transient stability prediction include (i) ease of input data capture, (ii) simplicity, speed and accuracy of input data processing, and (iii) accuracy of final decision making.

The input data used should allow for easy capture and transmission, in real-time, to a centralized point. This should also be done in a short-time window. Rotor angle [5], speed deviation [2], and bus voltage [4] are some of the input parameters that have been used. Using single input data type for each machine or bus is desired. Capturing multiple input data types presents implementation challenges. For example, the work presented in [6] uses 34 input features derived from generator electromagnetic powers, rotor angles and speeds, bus voltages and transmission line power flows, among others. Also, in [7], 10-12 input data samples per generator are required, and in [8], 4 inputs per generator are required. These data requirements will make the volume of data required for large systems huge. Also, the technique presented in [5] uses data captured in a rather long time-window of 120ms.

The processing of input data should be simple, fast and accurate. Significant success has been chalked in this area; but there is still room for improvement. For example, in [4], extensive dynamic simulations are required to establish the stability boundaries of each generator.

The use of pre-determined templates in decision making such as in [4], [9] and [10] is not helpful, considering the fact that changes in system topology may render such templates ineffective. Also, the technique in [11] requires a long period of up to 2.5 seconds after fault clearance to make a decision as to whether or not a system will be stable. Thus, there is the need for an improved transient stability status detection or prediction scheme.

Support vector machine (SVM), multilayer perceptron neural network (MLPNN) and Radial basis function neural network (RBFNN) are artificial intelligence (AI) techniques commonly used for decision making in power system studies. However, their performance in the prediction of transient stability status has not been compared. It is important to highlight

that there is an erroneous perception on the part of some researchers about AI techniques. Some researchers perceive them as black-box type decision making tools [4]. Contrary to this perception, AI techniques are based on sound mathematical principles. Their decisions (outputs) are mathematically determined from given inputs. This has been demonstrated in this paper.

This paper proposes an improved scheme to predict transient stability or otherwise and also compares the performance of the aforementioned AI tools. The scheme uses generator rotor angles as input data. The rotor angles are sampled at a rate of 60 samples per second. This sampling rate is practically feasible in the capture of rotor angles [13]. Also, phasor measurement units do operate at this sampling rate [14]. Only the first sampled rotor angle value of each generator is required by the scheme. For each sampled rotor angle value, the absolute value is extracted. The extracted absolute rotor angle values (one for each generator) are then summed. The summed value is then fed into one of the decision making tools which predicts the stability status.

Compared to schemes existing in literature, the proposed technique uses single input data for each generator, captured in a shorter time window ($1/60^{th}$ of a second), requires minimal training data (less than 2% of data generated), uses minimal input data (number of inputs equals number of generators), does not require predetermined templates, and its implementation does not require complex computations.

The rest of the paper is organized as follows: Section 2 discusses the use of rotor angle as input parameter. Section 3 discusses SVM, MLPNN and RBFNN. Section 4 presents the proposed scheme while Section 5 highlights the test system used and simulations done. Results obtained are presented and discussed in Section 6. Conclusions drawn are highlighted in Section 7.

2. USE OF ROTOR ANGLE AS INPUT PARAMETER

Rotor angle has been extensively used as power system input parameter for various studies. Rotor angle is a key parameter in the fundamental equation governing generator rotor dynamics [15]. The equation is given as [15]:

$$M\frac{d^2\delta}{dt^2} = P_m - P_e \tag{1}$$

where M is the inertia coefficient, δ is the rotor angle, P_m is the mechanical power and P_e is the electrical power. It can also be shown that [2],

$$\frac{d\delta}{dt} = \left[\frac{\omega_0}{H}\int_{\delta_0}^{\delta} P_a d\delta\right]^{\frac{1}{2}} \tag{2}$$

where H is the inertia constant and P_a is the difference between input mechanical power and output electromagnetic power. For stability to be attained after a disturbance, it is expected that $\frac{d\delta}{dt}$ will be zero in the first swing [15]. This condition gives rise to the equal area criterion which is a well-known classical transient stability criterion.

Rotor angles are normally expressed relative to a common reference. This reference cannot be based on a single generator, since any instability in the reference generator makes the relative angles meaningless. In order to overcome this difficulty, the concept of system centre of inertia (COI) angle is used to obtain a reference angle [9].

Many researchers discourage the use of rotor angles in algorithms [9]. This is because the COI values, in practice, require continuous updates using real time measurements. This requires extra pre-processing and has significant errors. However, recent work by engineers from Schweitzer Engineering Laboratories, Inc. and San Diego Gas & Electric point to a breakthrough in capturing rotor angle data [13]. The researchers [13] have successfully installed and commissioned a rotor angle measurement system on the generators in a 740 MVA combined cycle plant. No reference angle value is required in the measurement. This has offered a tremendous boost to the continuing use of rotor angles as input parameter for power system studies. This significant success motivated the use of rotor angle as input parameter in this work.

3. DECISION MAKING TOOLS

3.1. Support Vector Machine

Support vector machine (SVM) is an extremely powerful machine learning algorithm that focuses on classifying data [16], [17]. SVMs are inherently two-class classifiers. The main idea of a support vector machine is to construct a hyperplane as the decision surface in such a way that the margin of separation between two data categories is maximized. SVMs can be used when the data to be classified has two classes. They separate the data into two categories, namely positive (+1) and negative (-1).

SVMs can provide good generalization performance on pattern classification problems despite the fact that they do not incorporate problem-domain knowledge. This attribute is unique to SVMs [17]. In addition to using separating hyperplanes, SVMs use support vectors to aid in data classification. Support vectors are points that are closest to the separating hyperplane; these points are on the boundary of the slab [16]. The building of a support vector machine hinges on the following two mathematical operations: (a) nonlinear mapping of an input vector into a high-dimensional feature space that is hidden from both the input and the

output, and (b) construction of an optimal hyperplane for separating the features discovered in (a) [17].

Figure 1 illustrates these definitions, with + indicating data points of type 1, and – indicating data points of type –1 [18].

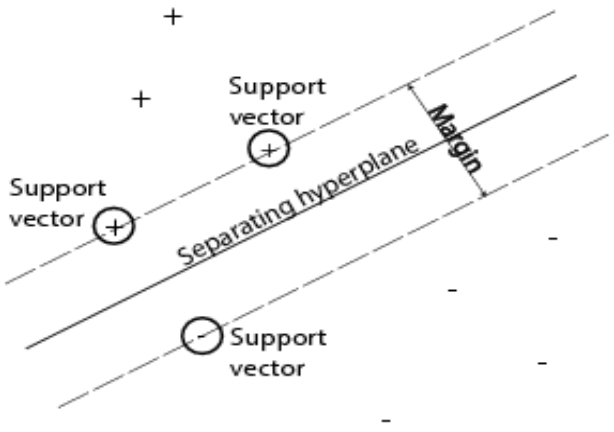

Fig. 1. Data points of SVM

Figure 2 shows the general architecture of an SVM [17]. The input layer consists of the input signal vector. In the hidden layer, an inner-product kernel is computed between the input signal vector (**x**) and support vector ($\mathbf{s_i}$). The linear outputs of the hidden layer neurons are summed in the output neuron. The output neuron has a bias.

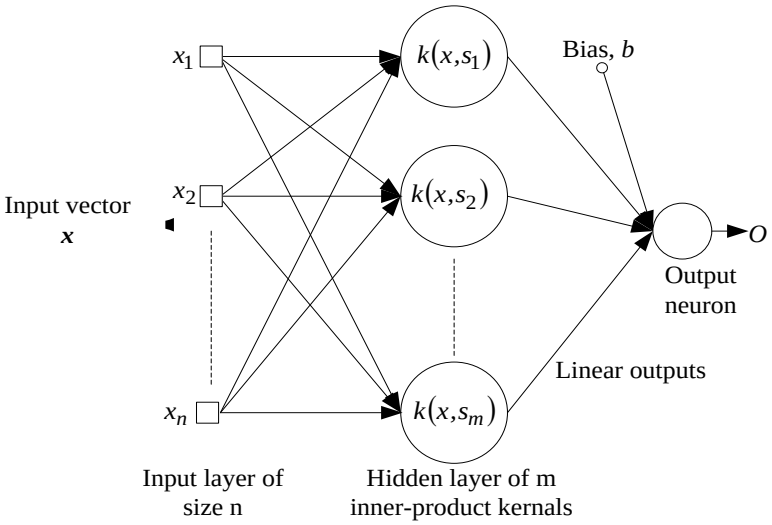

Fig. 2: General architecture of support vector machine

The interim output, O of a support vector machine can be computed as [18]:

$$O = \sum_i \mathbf{w}_i \, k(\mathbf{x}, \boldsymbol{s}_i) + b \tag{3}$$

where **x** is the input vector, $\mathbf{s}_i$ is the support vector, b is the bias, and $\mathbf{w}_i$ is the weight vector. The function $k(\mathbf{x}, \mathbf{s}_i)$ is a kernel of **x** and $\mathbf{s}_i$. The weight and bias values are obtained in the training phase. A linear kernel, meaning dot product, was used in this work. The linear kernel was selected because the classification required is a two-class one. Other possible kernel functions are quadratic, polynomial, Gaussian or radial basis function, and multilayer perceptron [18].

SVMs are trained with input-output pairs to give targets of either +1 or -1. An output of $+1$ is given when $O \geq 0$ while -1 is recorded when $O < 0$. In this work, the SVM was trained to produce a target of +1 for a condition that will lead to transient stability and -1 for a condition that will lead to transient instability. In other words, stability status, *t,* from SVM output, *O* is obtained as follows:

$$O \geq 0 \quad \Rightarrow \quad t = +1 \Rightarrow system\ is\ stable \tag{4}$$

$$O < 0 \quad \Rightarrow \quad t = -1 \Rightarrow system is unstable \tag{5}$$

The training was done using the sequential minimal optimisation method [16].

3.2. Multilayer perceptron and Radial basis function neural networks

Artificial Neural Networks (ANNs) mimic the human brain and have remarkable ability to derive meaning from complicated or imprecise data. They can be used to extract patterns and detect trends that are too complex to be noticed by humans or other computer techniques [19]. Two commonly used neural networks are radial basis function (RBF) and multilayer perceptron (MLP) neural networks [20], [21].

3.2.1. Multilayer perceptron neural network

Multilayer perceptron neural network is one of the artificial neural networks that have gained wide application in power system studies [22], [5]. It can be used to extract patterns and detect trends that are too complex to be noticed by humans or other computer techniques [22], [5]. Typically, the MLPNN is organized as a set of interconnected layers of artificial neurons, namely input, hidden and output layers. When a neural group is provided with data through the input layer, the neurons in this first layer propagate the weighted data and randomly selected bias, through the hidden layers. Once the net sum at a hidden node is determined, an output response is provided at the node using a transfer (activation) function. Commonly used transfer functions are: linear, log-sigmoid and hyperbolic tangent sigmoid [23], [24]. MLPNN, like any other neural network, has to be trained [23]. In this work, the MLPNN was trained using the Levenberg–Marquardt algorithm [25].

The MLPNN used in this work has the architecture shown in *Fig. 3*.

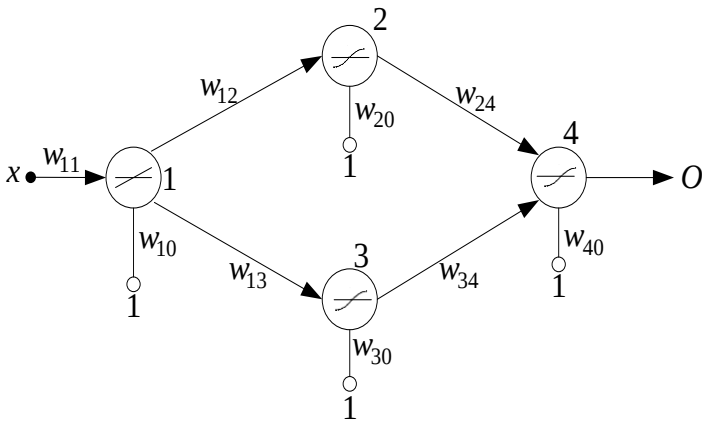

Fig. 3: Architecture of used MLPNN

where x is the input data, w_{ij} is the weight between neurons i and j, w_{i0} is the weight of the bias of neuron i, and O is the output of the neural network. Biases have fixed input values of 1. The input neuron has linear transfer functions while the hidden layer and output neurons have tangent sigmoid transfer functions. The output O of the MLPNN is determined as follows:

The output, y_1, of neuron 1 is given by:

$$y_1 = f\left(xw_{11} + w_{10}\right) = xw_{11} + w_{10} \tag{6}$$

The output, y_2, of neuron 2 is given by:

$$\begin{aligned} y_2 &= f\left(y_1 w_{12} + w_{20}\right) \\ &= \frac{e^{2\left(y_1 w_{12} + w_{20}\right)} - 1}{e^{2\left(y_1 w_{12} + w_{20}\right)} + 1} \\ &= \frac{e^{2\left(\left(xw_{11} + w_{10}\right)w_{12} + w_{20}\right)} - 1}{e^{2\left(\left(xw_{11} + w_{10}\right)w_{12} + w_{20}\right)} + 1} \end{aligned} \tag{7}$$

The output, y_3, of neuron 3 is given by:

$$\begin{aligned} y_3 &= f\left(y_1 w_{13} + w_{30}\right) \\ &= \frac{e^{2\left(y_1 w_{13} + w_{30}\right)} - 1}{e^{2\left(y_1 w_{13} + w_{30}\right)} + 1} \\ &= \frac{e^{2\left(\left(xw_{11} + w_{10}\right)w_{13} + w_{30}\right)} - 1}{e^{2\left(\left(xw_{11} + w_{10}\right)w_{13} + w_{30}\right)} + 1} \end{aligned} \tag{8}$$

The output, O, of MLPNN is thus given by:

$$O = f\left(w_{24}y_2 + w_{34}y_3 + w_{40}\right) = \frac{e^{2\left(w_{24}y_2 + w_{34}y_3 + w_{40}\right)} - 1}{e^{2\left(w_{24}y_2 + w_{34}y_3 + w_{40}\right)} + 1} \tag{9}$$

The MLPNN was trained to give an output of 0 if a disturbance will lead to transient stability, and an output of 1 if a disturbance will result in transient instability.

In practice, neural networks do not always give exact outputs of 0 or 1. For example, an expected output of 0 may be presented as 0.017 while a value of say 0.819 may be obtained instead of 1. As a result, in this work, (10) and (11) are used to round the output of the MLPNN to either 0 or 1.

$$O \geq 0.5 \rightarrow O = 1 \tag{10}$$

$$O < 0.5 \rightarrow O = 0 \tag{11}$$

3.2.2. Radial basis function neural network

Radial basis function neural network (RBFNN) is also an extremely powerful neural network [26]. It is a two-layered neural network having an input (or hidden) layer and output layer. The neurons in the input layer have Gaussian transfer function while those in the output layer have linear transfer function. The number of neurons in the output layer is predetermined by the user. The number of input neurons is however determined in the training process. Fig. 4 shows the architecture of a RBFNN with one input and one output.

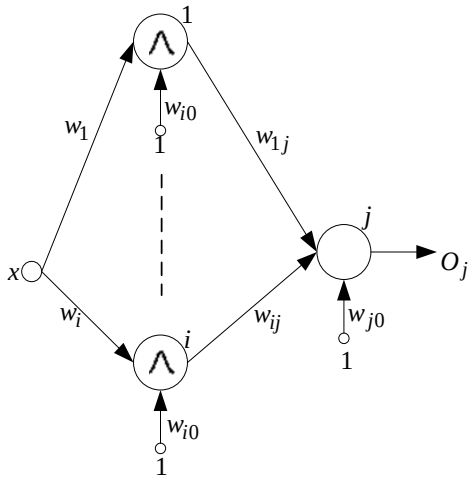

Fig. 4: Architecture of RBFNN

The output Y_i of a radial basis neuron *i* in the input (or hidden) layer can be obtained as [26]:

$$Y_i = R\left(\left\|w_i.x\right\|w_{i0}\right) \tag{12}$$

where x is the input vector (signal), w_i is the weight vector of radial neuron i, $\|w_i.x\|$ is the Euclidean distance between the two vectors, w_{i0} is the bias weight of neuron i, and R is a Gaussian function. In MATLAB, R is given as [27]:

$$R(n) = e^{-n^2} \tag{13}$$

The output O_j of neuron j in the output layer is given as:

$$O_j = Y_i w_{ij} + w_{j0} \tag{14}$$

where w_{ij} is the weight of the connection between neuron i in the input layer and neuron j in the output layer, and w_{j0} is the bias weight of neuron j. The RBFNN was trained to give an output of 0 if a disturbance will lead to transient stability, and an output of 1 if a disturbance will result in transient instability.

4. PROPOSED TRANSIENT STABILITY STATUS PREDICTION SCHEME

Figure 5 shows a functional block diagram of the proposed technique. The scheme is activated upon a large disturbance such as the tripping of a loaded line, generator or transformer and operates by sampling the rotor angle of each generator in the system using a sampling rate of 60 samples per second. It then extracts only the first sample of each generator. The absolute value of each extracted sample is then obtained. The obtained absolute values are then summed and used as input to a trained decision-making tool (which is either SVM, MLPNN or RBFNN). The decision-making tool then outputs the predicted transient stability status of the system.

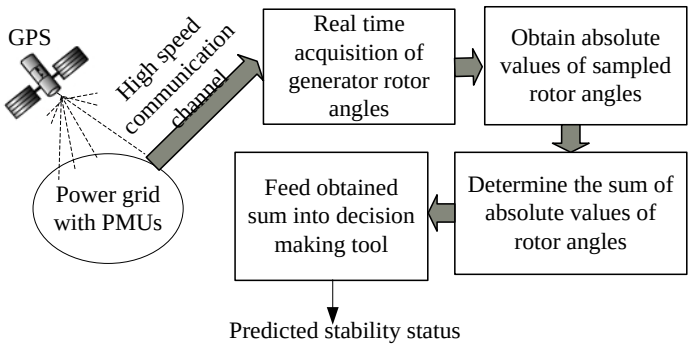

Fig. 5: Functional block diagram of the proposed technique

The operating procedure is further outlined as follows:

- For every generator *i*, sample the rotor angle and extract only the first rotor angle sample, δ_i:

$$\delta_i = \delta_{i,1} \quad i = 1,2,...,N \tag{15}$$

where N is the number of generators of the system

- For each extracted rotor angle sample, obtain the absolute value $|\delta_i|$.
- Obtain the input, *x*, to the decision making tool (MLPNN, RBFNN or SVM) by summing the absolute values as follows:

$$x = \sum_{i=1}^{N} |\delta_i|, \quad i = 1,2,...,N \tag{16}$$

5. TEST SYSTEM USED

The IEEE 39-bus test system was used to test the proposed scheme. It is shown in Fig. 6.

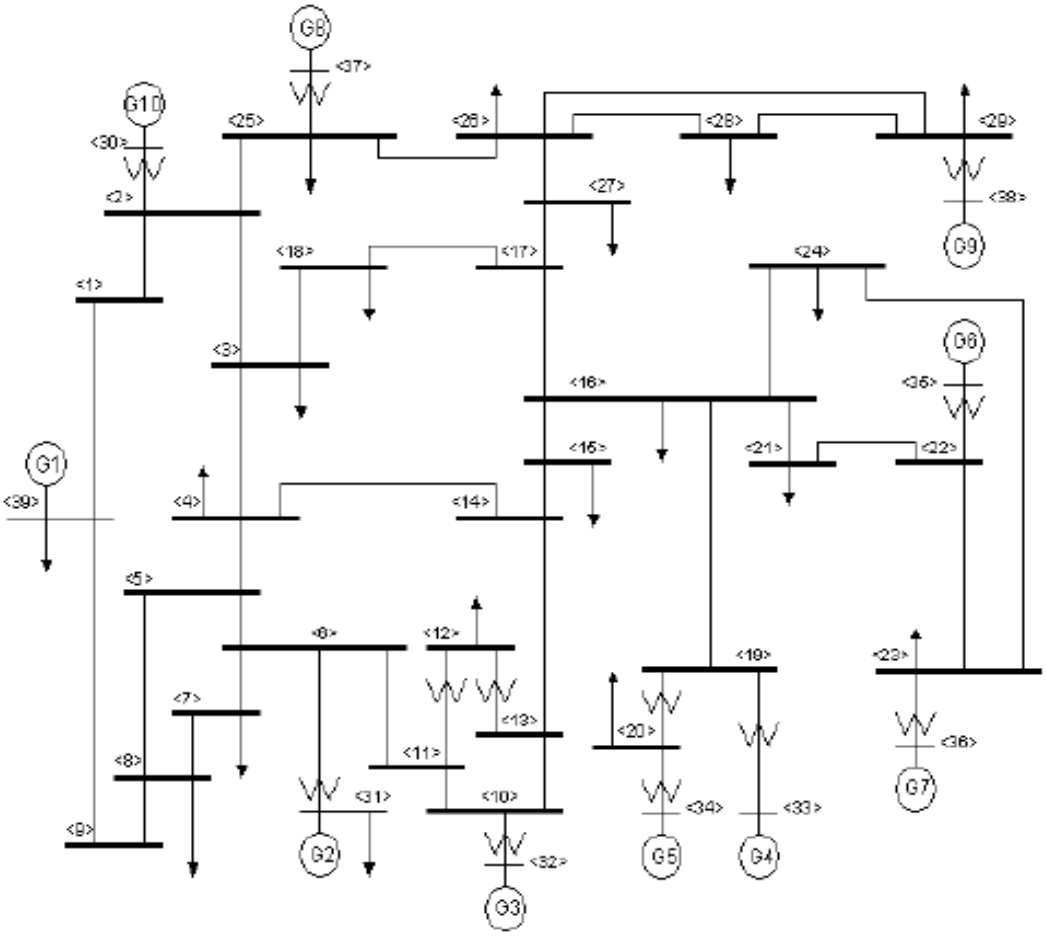

Fig. 6: IEEE 39-bus test system

This test system, also known as the New England test system, is a very popular test system for transient stability studies. Several researchers have used it for their work [4], [9], [10] for these main reasons: it is a model of a practical system; and it can be modeled and simulated using several non-commercial versions of simulation tools. The system consists of 10 generators, one of which is a generator representing a large system. Data for its model was obtained from [28], [29].

Transient stability analysis of the test system was performed using the PSS®E software. A detailed dynamic model which includes prime mover and excitation system dynamics was used. Several fault simulations were obtained by varying the fault location, fault duration, system loading, network topology, and generator availability.

About fault location, bus and line faults at different locations were simulated. Fault durations were also varied by starting with short durations which resulted in transient stability and extending them gradually until instability occurred. The effect of shutting down a generator due to low loading conditions or for purposes of maintenance was also considered. For example, for a loading level of 80% base load, generator 2 (G2) was removed from circuit before disturbances were applied. Additionally, the effect of changes in network topology was investigated by considering N-1 contingency. For example, for some of the simulations, the line between bus 25 and bus 26 was removed before the application of faults.

A total of 210 fault simulations were done to obtain 105 cases of transient stability and 105 cases of transient instability. The following criterion was used to determine the stability status of the system following a simulated disturbance: A system was seen as being transiently unstable if the rotor angle difference between any two generators exceeded 180 degrees within a typical study period of 3 seconds following fault clearance, otherwise, the system was seen to be stable [3].

Sampling of rotor angles was done allowing for a trigger delay time of 2 ms after fault clearance. The sampling and analysis of data were done using the MATLAB software.

6. RESULTS OBTAINED

6.1. Rotor angle trajectories

Two representative cases are presented here to show rotor angle trajectories obtained for the simulated cases. *Figure 7* shows time responses of rotor angles for a case of transient stability. The fault was applied on the line between buses 13 and 14 of the test system at 110% base loading. The fault was applied at $t = 0.1s$ and the line tripped at $t = 0.2s$. Figure 8 shows time responses of rotor angles for an unstable case. The system and fault conditions were the same as those for the stable case except that the fault duration was extended by 0.2 seconds to make the system transiently unstable. *Table 1* shows absolute values of sampled

rotor angles for each machine for the two fault cases.

The input to decision making tool using (16) is obtained as follows:

$$x(stable) = 103.1633$$

$$x(unstable) = 350.2648$$

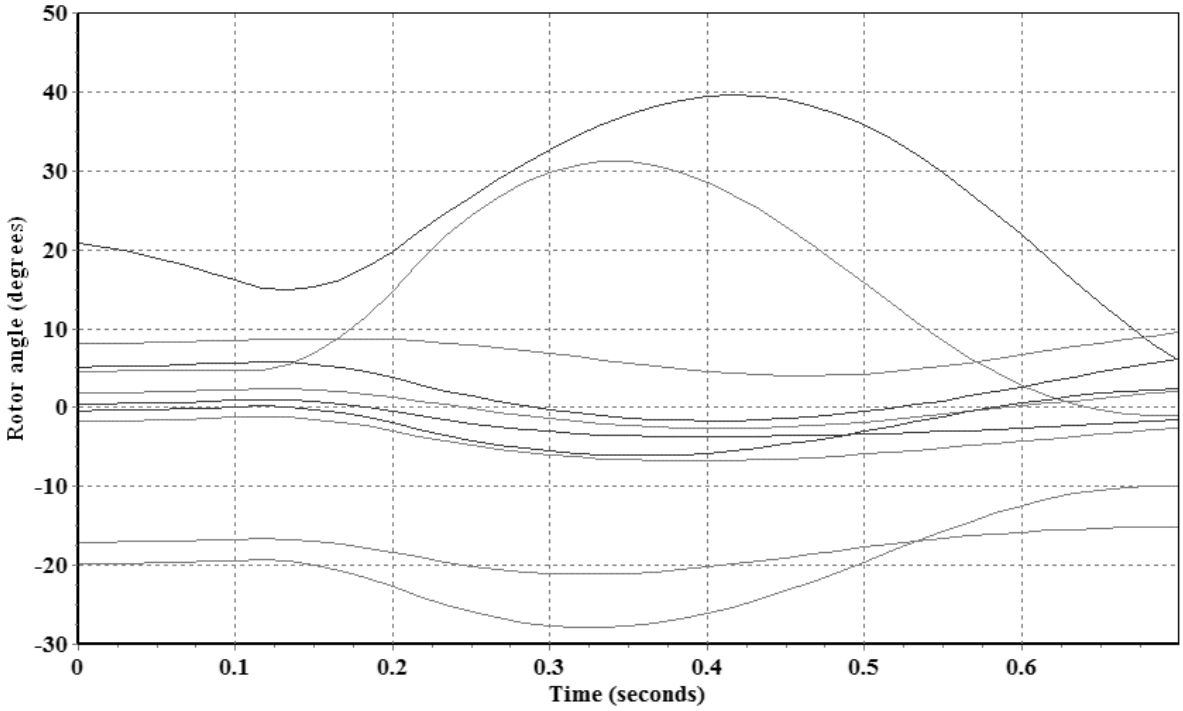

Fig. 7: Rotor angle trajectories for a stable condition

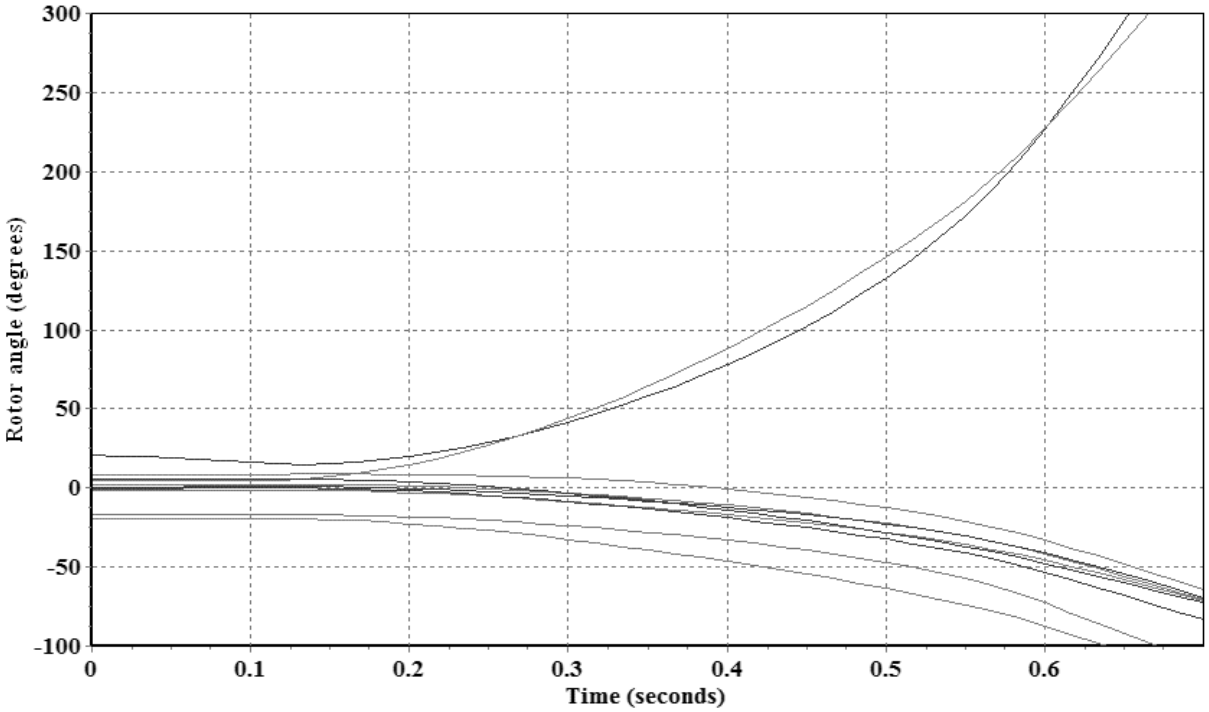

Fig. 8: Rotor angle trajectories for an unstable condition

Table 1: Absolute values of sampled rotor angles

Generator	Absolute values of rotor angles (degrees)	
	Stable	Unstable
1	23.9276	49.0633
2	22.2254	85.5155
3	18.3866	96.6407
4	0.8698	12.5067
5	3.6542	18.5483
6	8.4008	2.2257
7	1.0094	13.7294
8	2.7970	20.8451
9	2.9092	16.0681
10	18.9833	35.1220

6.2. Support vector machine (SVM)

6.2.1. Training

Rotor angle data from two cases of transient stability, and two cases of transient instability, representing 1.90% of data generated, were used to train the SVM. The remaining 98.10% of the data generated (103 cases of instability and another 103 cases of stability) were then used to test the proposed scheme. The training data of 1.90% is very low when compared with the training data of 75% used for some stability status prediction schemes existing in literature [9].

6.2.2. Structure of SVM

The characteristic data of the SVM after training is presented below:

$$\text{Support vector, } s_i = \begin{pmatrix} 145.1524 \\ 167.7435 \end{pmatrix}$$

$$\text{Weight vector, } w_i = \begin{pmatrix} 0.0039 \\ -0.0039 \end{pmatrix}$$

$$\text{Bias, } b = 13.8504$$

For the above SVM structure, the interim output, O given by (3) becomes

$$\begin{aligned} O(x) &= x(s_1 \times w_1 + s_2 \times w_2) + b \\ &= x(145.1524 \times 0.0039 + 167.7435 \times -0.0039) \\ &\quad + 13.8504 \\ &= -0.08811x + 13.8504 \end{aligned} \tag{17}$$

6.2.3. Performance

The prediction accuracy of the scheme using SVM as decision making tool was found to be 100%. A sample calculation of the SVM output is presented using input value, *x*, obtained from *Table 1*.

Transient stable case

Interim output, *O*, of SVM using (17) is obtained as:

$$O(x=103.1633) = -0.08811 \times 103.1633 + 13.8504 = 4.7607 \quad (18)$$

Stability status, t, using (4) is +1 which means transient stable.

Transient unstable case

Interim output, O, of SVM using (17) is obtained as:

$$O(x=350.2648) = -0.08811 \times 350.2648 + 13.8504 = -17.0114 \quad (19)$$

Stability status, t, using (5) is -1 which means transient unstable.

6.3. Multilayer perceptron neural network (MLPNN)

6.3.1. Training

Initially, the MLPNN was trained with the same data used to train the SVM. However, this did not yield satisfactory test results. Desired performance was achieved only after training with higher volume of training data; which is 4.76% of total generated data.

6.3.2. Architecture of MLPNN

The MLPNN had three layers (as shown in *fig. 3*). The input layer had one neuron with a linear transfer function while the hidden layer had 2 neurons with tangent sigmoid transfer functions. The output layer had one neuron, also with a tangent sigmoid transfer function. The characteristic data is presented in *Table 2*.

Table 2: Weight values of MLPNN

Input signal – Input layer	Input layer – Hidden layer	Hidden layer – output
$w_{11} = -4.882$	$w_{12} = -5.892$	$w_{24} = 6.864$

$w_{10} = -2.7$	$w_{13} = 2.7856$ $w_{20} = 3.8567$ $w_{30} = 2.829$	$w_{34} = -0.25914$ $w_{40} = 0.32231$

6.3.3 Performance

Applying (6) to (9), the MLPNN outputs are obtained as follows:

Transient stable case

$$O(x = 103.1663) = 0.0000012 \tag{20}$$

Using (11), *O* is 0 which means transient stable.

Transient unstable case

$$O(x = 350.2648) = 1 \tag{21}$$

This means that the system will be transient unstable.

6.4. Radial basis function neural network (RBFNN)

The RBFNN was also initially trained with the same input data used to train the SVM. However, this did not yield satisfactory performance. The highest performance of 63% prediction accuracy was obtained only after increasing the volume of training data samples to 9.05% of total data. Beyond this, it was observed that the prediction accuracy remained the same. Thus, the RBFNN offered poor performance.

7. CONCLUSION

A novel technique for real-time prediction of transient stability status has been presented. The technique does not require any large volume of input data. The data processing approach is also simple. Its operation is also fast considerating the fact that it requires minimal input data captured in a very short time window. It can also be easily implemented. The performance of three artificial intelligence decision making tools namely support vector machine, multilayer perceptron neural network, and radial basis function neural network have also been evaluated. The support vector machine has been found to be most effective followed by the multilayer perceptron neural network. The radial basis function neural network gave the least performance.

REFERENCES

[1] U.S.-Canada Power System Outage Task Force, *Final Report on the August 14, 2003 Blackout in the United States and Canada: Causes and Recommendations*, Apr. 2004. Available: http://www.nerc.com/filez/blackout.html

[2] E. A. Frimpong, A. Johnson, and P. Y. Okyere, *Neural network and speed deviation based generator out-of-step prediction scheme*, Journal of Electrical Engineering, vol.15, no.2, pp.1-8, June 2015.

[3] P. Kundur, J. Paserba, V. Ajjarapu, G. Andersson, A. Bose, C. Canizares, N. Hatziargyriou, D. Hill, A. Stankovic, C. Taylor, T. Van Cutsem, and V. Vittal: *Definition and classification of power system stability*, IEEE Transactions on Power Syststems, vol. 19, no. 2, pp. 1387–1401, May 2004.

[4] D. R. Gurusinghe and A. D. Rajapakse, *Post-disturbance transient stability status prediction using synchrophasor measurements*, IEEE Transactions on Power Systems, vol. 31, no. 5, pp. 3656-3664, Sept. 2016.

[5] N. Amjady and S. F. Majedi, *Transient stability prediction by a hybrid intelligent system*, IEEE Transaction on Power Systems, vol. 22, no. 3, pp. 1275 -1283, August 2007.

[6] Y. Zhou, J. Wu, Z. Yu, L Ji. and L. Hao, A *hierarchical method for transient stability prediction of power systems using the confidence of a svm-based ensemble classifier*, Energies, vol. 9, pp. 1-20, 2016.

[7] J. Hazra, R. K. Reddi, K. Das, D. P. Seetharam and A. K. Sinha, *Power grid transient stability prediction using wide area synchrophasor measurements*, Proceeding of 3rd IEEE PES Innovative Smart Grid Technologies Europe (ISGT Europe), Berlin, China, pp. 1-8, 2012.

[8] A. N. AL-Masri, M. Z. A. A. Kadir, H. Hizam and N. Mariun, A *novel implementation for generator rotor angle stability prediction using an adaptive artificial neural network application for dynamic security assessment*, IEEE Transactions on Power Systems, vol. 28, no.3, p. 2516-2525, 2013.

[9] A.D. Rajapakse, F. Gomez, O.M.K.K. Nanayakkara, P.A. Crossley and V.V. Terzija, *Rotor angle stability prediction using post-disturbance voltage trajectory patterns*, IEEE Transactions on Power Systems, vol. 25, no. 2, pp. 945-956, 2010.

[10] F. Gomez, A. Rajapakse, U. Annakkage and I. Fernando, *Support vector machine-based algorithm for post-fault transient stability status prediction using synchronized measurements*, IEEE Transactions on Power Systems, vol. 26, no. 3, pp. 1474-1483, 2011.

[11] T. Guo, and J. V. Milanović, O*n-line prediction of transient stability using decision tree method — sensitivity of accuracy of prediction to different uncertainties*, Proceedings of the IEEE Grenoble PowerTech, Grenoble, 2013.

[12] D. E. Echeverría, J. L. Rueda, J. C. Cepeda, D. G. Colomé and I. Erlich, *Comprehensive approach for prediction and assessment of power system transient stability in real-time*, Proceedings of the 4th IEEE PES Innovative Smart Grid Technologies Europe (ISGT Europe), Copenhagen, pp. 1-5, 2013.

[13] T. Rahman, S. Sankaran, N. Seeley and K. Garg, *Capturing generator rotor angle and field*

quantities – SDG&E experience and approach to using nontraditional generator measurements, Proceedings of the 42nd Annual Western Protective Relay Conference, Spokane, Washington, p. 1-9, 2015.

[14] *IEEE Standard for Synchrophasor Measurements for Power Systems*, IEEE Std. C37.118.1-2011, Dec. 2011.

[15] I. J. Nagrath and D. P. Kothari, *Power System Stability*, Power System Engineering, New Delhi, India; Tata Mcgraw-Hill, ch. 12, sec. 12.2, pp. 486-489, 1994.

[16] Statistics and Machine Learning Toolbox™, User's Guide, Matlab R2015a.

[17] Support Vector Machine [Online]. Available: https://www.fer.unizg.hr /_download/repository/ 07-SupportVectorMachine, 2016.

[18] Matrix Laboratory software, MATLAB R2013a.

[19] C. W. Liu, M. C. Su, S. S. Tsay, and Y. J. Wang, *Application of a novel fuzzy neural network to real-time transient stability swings prediction based on synchronized phasor measurements*, IEEE Transactions on Power Syststems, vol 14, no. 2, pp. 685-692, May 1999.

[20] K. J, McGarry, S. Wermter and J. MacIntyre, *Knowledge extraction from radial basis function networks and multi-layer perceptrons*, International Joint Conference on Neural Networks, Washington D.C., p. 1-4, 2009.

[21] A. Kavousifard and H. Samet, *Consideration effect of uncertainty in power system reliability indices using radial basis function network and fuzzy logic theory*, *Neurocomputing*, vol. 74, no. 17, pp. 3420-3427, 2011.

[22] E. A. Frimpong, J. A. Asumadu and P.Y. Okyere, S*peed deviation and multilayer perceptron neural network based transient stability status prediction scheme*, Journal of Electrical and Electronic Engineering, vol. 15, no. 2, pp. 9-16, 2015.

[23] A. N. Fathian, and M.R. Gholamian, *Using MLP and RBF neural networks to improve the prediction of exchange rate time series with ARIMA*, International Journal of Information and Electronics Engineering, vol. 2, no. 4, pp. 543-546, 2012,

[24] H. Memarian, and S. K. Balasundram, C*omparison between multi-layer perceptron and radial basis function networks for sediment load estimation in a tropical watershed*, Journal of Water Resource and Protection, vol. 4, pp. 870-876, 2012.

[25] H. Yu, and B. M. Wilamowski, *Intelligent Systems*, Industrial Electronics Handbook, 2nd Edition, CRC press, pp. 12-1 to 12-15, 2011.

[26] A. Kavousifard and H. Samet: *Consideration effect of uncertainty in power system reliability indices using radial basis function network and fuzzy logic theory*, Neurocomputing, vol. 74, No. 17, 2011, p. 3420-3427.

[27] M. H. Beale, M. T. Hagan and H. B. Demuth, *Neural Network Toolbox™, User Guide*, MATLAB, R2016b, pp. 6-3 – 6-4, 2016.

[28] E. A. Frimpong: P*rediction of transient stability status and coherent generator groups*, PhD dissertation, Dept. of Elect. and Elec. Eng., Kwame Nkrumah University of Science and Technology, Kumasi, Ghana, 2015. [Available online]

[29] Y. Song, *Design of secondary voltage and stability controls with multiple control objectives*, PhD dissertation, Sch. of Elect. and Compt. Eng., Georgia Institute of Technology, Georgia, USA, 2009. [Available online]